THE JOURNAL OF PHYSICAL CHEMISTRY Letters

LETTER

pubs.acs.org/JPCL

How Toxic Are Ionic Liquid/Acetonitrile Mixtures?

Vitaly V. Chaban* and Oleg V. Prezhdo

Department of Chemistry, University of Rochester, Rochester, New York 14627, United States

Supporting Information

ABSTRACT: Acetonitrile (ACN) is suggested to be a cosolvent of room-temperature ionic liquids (RTILs) in order to decrease their unprecendented viscosity and increase ionic transport. Nevertheless, apart from its doubtless virtues, ACN possesses moderate toxicity to animals due to its high volatility at medium temperatures and subsequent ability to form highly toxic compounds, including cyanogen. Because of these considerations, ACN has been recently banned in a series of commercial applications. In turn, RTILs are usually positioned as nontoxic, green solvents, mainly due to their negligible volatility. This Letter investigates the volatility of the imidazolium-based RTILs/ACN mixtures, where RTILs are represented by 1-ethyl-3-methylimidazolium tetrafluoroborate and 1-butyl-3-methylimidazolium tetrafluoroborate. On the basis of the atomistic precision simulations of liquid/vapor interfaces over a wide composition range, we evidence that RTILs are able to noticeably decrease the volatility of ACN, and hence, reduce a hazard. The reported data favor wide technological applications of RTILs/ACN mixtures.

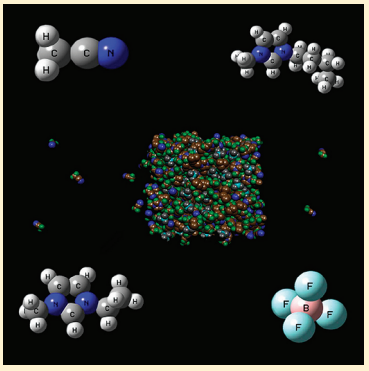

SECTION: Atmospheric, Environmental and Green Chemistry

Both room-temperature ionic liquids[1−4] (RTILs) and acetonitrile (ACN) are of great importance and research interest for chemical industry and fundamental studies.[5−9] Recently, the mixtures of these organic liquids[10−12] have been suggested as a novel high-performance electrolyte for a variety of applications, including lithium-ion batteries, solar cells, and supercapacitors. Indeed, RTILs comprise exclusively ions, and therefore potentially possess extremely high ionic conductivity. Unfortunately, the viscosity of RTILs is also unusually large,[13] normally exceeding 50−100 cP at room temperature.[14] It leads to a glass-like behavior of the substance, which exhibits low self-diffusion resulting in a relatively small conductivity.[15] The addition of the low-viscous aprotic liquid, which is thereunto well miscible with RTILs, considerably enhances ionic mobility.[16] On the basis of its well-known physical and electrochemical properties, ACN is one of the strongest candidates of such cosolvent.

While the above composition provides a high-performance electrolyte, there still stands an important problem of ACN toxicity. ACN is an Environmental Protection Agency (EPA)-classified toxic waste possessing a constant hazard for humans due to its significant volatility at room temperature and low boiling point (82 °C). The inhalation of the ACN vapors can cause asphyxia, nausea, vomiting, and tightness of the chest. Furthermore, ACN is able to form a range of highly toxic compounds, including cyanogen. On the basis of these considerations, ACN has been recently banned in a series of commercial applications. Although there are naturally a variety of general possibilities for individuals to be exposed to ACN, the primary source is breathing contaminated air.

In this Letter, we present the first atomistic simulation study of the potential toxicity/hazard of the imidazolium-based[17] RTIL/ACN mixtures. We assume that overall toxicity in this case is preferentially associated with a volatility of ACN. In turn, RTILs are known for their negligible volatility and are often positioned as safe solvents of the future.[18] Apart from a narrow applied interest, the description of the liquid/vapor interfaces of the mixtures, containing two nearly opposite liquids, is of certain fundamental importance. This problem has never been considered before on the atomistic level.

We apply classical equilibrium molecular dynamics (MD) simulations with pairwise phenomenological interaction potentials to investigate the structure of liquid/vapor interfaces and saturated vapor pressure in the mixtures of 1-ethyl-3-methylimidazolium tetrafluoroborate ([EMIM][BF_4]) and ACN and 1-methyl-3-butylimidazolium tetrafluoroborate ([BMIM][BF_4]) and ACN over a wide composition range. The simulated systems are listed in Table 1 and represent the entire diapason of concentrations. The volatilities of liquids can be conveniently characterized via the saturated vapor pressures (Figure 1) as a function of ambient temperature, T.

Fortunately, although the force field model for ACN was not parametrized to reproduce the normal boiling point, it performs quite well. The corresponding error is about 5 K. At $T < 310$ K, all pressures are below 0.3 bar. After this point, the vapor pressure increases drastically, except for the RTIL-rich mixtures. The functional dependence of the saturated pressure versus temperature is traditionally described using Antoine's equation, $P_{sat} = \exp\{A - [B/(C + T)]\}$, containing three empirical parameters,

Received: August 29, 2011
Accepted: September 19, 2011
Published: September 19, 2011

Table 1. The Summary of the Simulated Systems Representing [EMIM][BF_4]/ACN and [BMIM][BF_4]/ACN Mixtures[a]

x_1, %	N (RTIL)	N (ACN)	N_{atoms} (em)	N_{atoms} (bm)	V_{sys} (em)	V_{sys} (bm)
0	0	400	2400	2400	229.3	229.3
10	30	270	2340	2490	202.0	204.0
25	75	225	3150	3525	232.3	244.7
50	150	150	4500	5250	277.8	304.8
75	225	75	7200	6975	323.5	365.0
90	270	30	6660	8010	351.6	395.0

[a] x_1 denotes the molar fraction of RTIL in the mixture, N(RTIL) and N(ACN) are the amounts of the corresponding particles, N_{atoms}(em), N_{atoms}(bm) and V_{sys}(em), V_{sys}(bm) are the total numbers of atoms and volumes of the systems for the [EMIM][BF_4]/ACN and [BMIM][BF_4]/ACN mixtures, respectively.

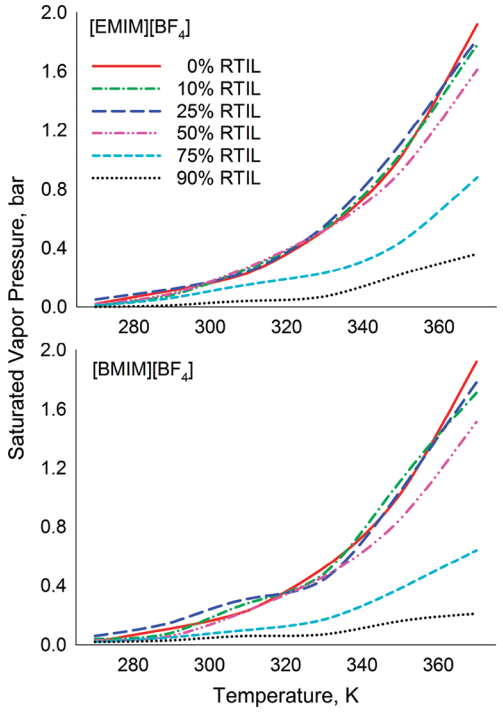

Figure 1. The saturated vapor pressure of the [EMIM][BF_4]/ACN and [BMIM][BF_4]/ACN mixtures over the temperature range 270−370 K.

A, *B*, *C*. These parameters are normally different under and above the boiling point of the respective liquid. Very surprisingly, the mixtures containing 10, 25, and 50% of RTIL exhibit only less than a 15% pressure decrease versus bulk ACN. Keeping in mind that the maximum of ionic conductivity is found at 5% < x(RTIL) < 25% (over the temperature interval 278−323 K), it should be clear that correlation between transport properties and vaporization is not tight, although obviously present. A sharp pressure decrease is observed only at x(RTIL) ≥ 75%, where the boiling point of ACN is not achieved even at 370 K. In these mixtures, the ACN particles are densely buried among the counterions, much higher temperatures being required to overcome the potential barriers preventing vaporization. Upon comparison,

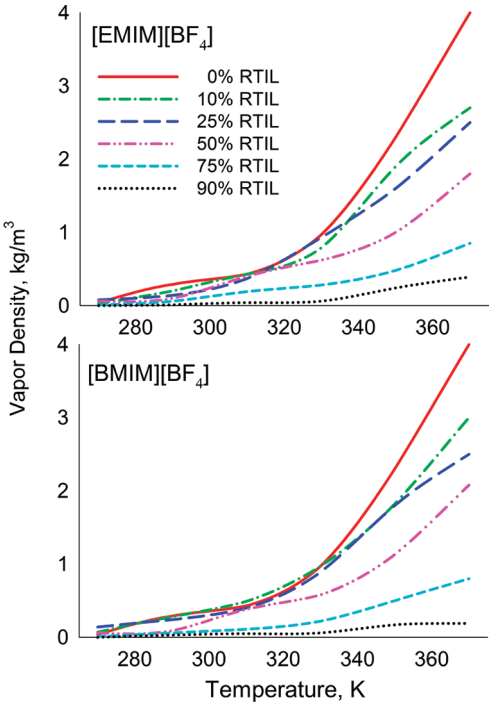

Figure 2. The density of the gaseous ACN upon the [EMIM][BF_4]/ACN and [BMIM][BF_4]/ACN mixtures over the temperature range 270−370 K.

the difference between 50% RTIL and 75% RTIL mixtures is ca. 5 times larger than that between 0% and 50% RTIL mixtures.

The gaseous phase above mixtures is formed exclusively by the ACN molecules, whose density (Figure 2) reaches 3 kg m^{-3} for 10% RTIL at 370 K. This property also exhibits a more precise dependence on the molar fraction of both RTILs than pressure. Upon comparison, the density of vapor for 75% [BMIM][BF_4] at 330 K is 0.2 kg m^{-3}, whereas the standard density of dry air at sea level is 1.225 kg m^{-3} (T = 288 K). Apparently, the influence of RTIL on the gaseous phase of ACN is huge; however, it is unexpectedly observed only in the RTIL-rich mixtures. The simulated fraction of RTILs in vapor is exactly zero, i.e., no ion leaves the condensed phase during 20 000 ps of MD simulations. A negligible volatility of RTILs is one of their most remarkable features, which is more characteristic for solids rather than liquids. The observed unusual composition of the vapor phase upon the RTIL/ACN mixtures may be important to understand the experimental heats of vaporization. Unlike the case of similar liquids, one cannot assume that the liquid and vapor phases of the RTIL/ACN mixtures have the same composition. Thus, the classical formula for vaporization heat should be modified in order to account for the absence of ions in the vapor phase at room temperature. The difference between [EMIM][BF_4] and [BMIM][BF_4] is quite insignificant, except at x(RTIL) ≥ 75%, where the difference exceeds 50%, [BMIM][BF_4]/ACN exhibiting lower pressure (Figure 2).

To summarize, 2-fold and even larger decreases of volatility of the RTIL/ACN mixtures are found to occur at x(RTIL) ≥ 75%. Per se, this finding looks positive, since it predicts a reduced ACN hazard. Although the ionic transport of the imidazolium-based RTILs at these compositions is relatively slow, the conductivity is, nevertheless, often higher than that of conventional electrolytes. For instance, the 75% [EMIM][BF_4]/ACN mixture shows

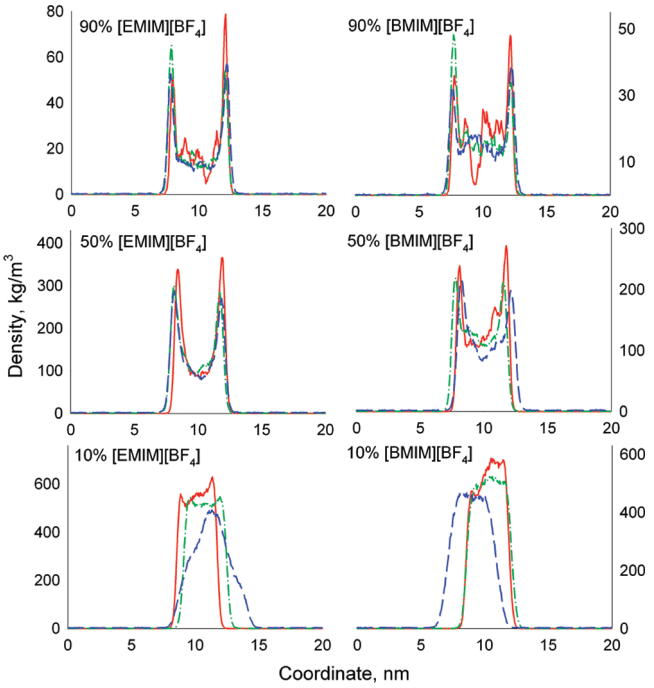

Figure 3. The partial densities of ACN in the [EMIM][BF_4]/ACN and [BMIM][BF_4]/ACN mixtures across the liquid/vapor interface at 290 (red solid), 330 (green dash-dotted), and 370 K (blue dashed).

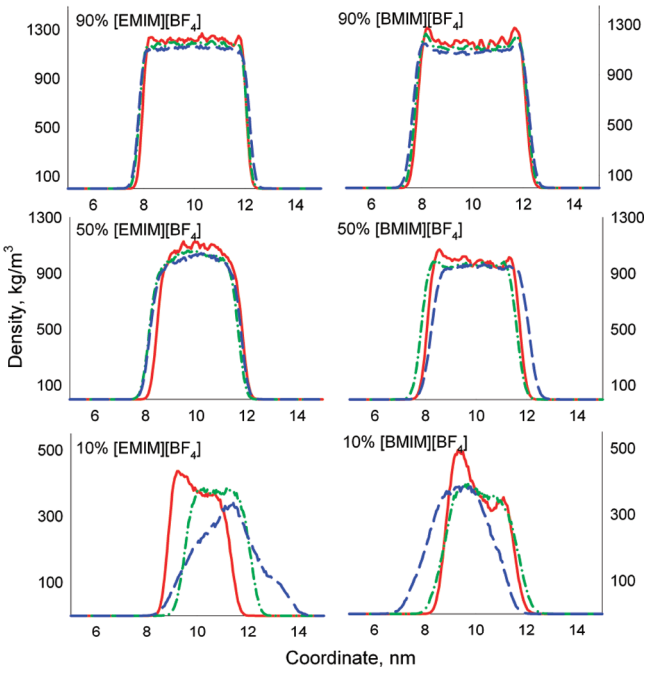

Figure 4. The partial densities of ionic liquid in the [EMIM][BF_4]/ACN and [BMIM][BF_4]/ACN mixtures across the liquid/vapor interface at 290 (red solid), 330 (green dash-dotted), and 370 K (blue dashed).

1.4−3.1 S/m conductivity at 298−323 K.[16] It is useful to establish a fine balance between high enough conductivity and low enough volatility of the mixture. The revealed possibility of this tuning opens an important avenue to improve the RTIL/ACN-containing electrolytes.[11,16]

Using the classical MD method opens a tremendous set of possibilities to perform atomistic precision experiments in order to find coveted trends and correlations. These experiments should not be necessarily physical themselves. Even more fruitful are tests that do not correspond to any realistic case, meanwhile unveiling a deeper understanding of the phenomenon and its applicability. In order to systematize the influence of the properties of ionic liquid on the volatility of ACN, we conduct the following experiment. The temperature of [EMIM][BF_4] is maintained constant at 270 K using a relatively tight response constant (0.1 ps), whereas ACN molecules are coupled at noticeably higher temperatures (330, 350, 370 K). The resulting saturated vapor pressures are 0.4, 0.7, and 0.8 bar. The resulting densities of the gaseous ACN are 0.17, 0.26, and 0.34 kg/m^3. Such a significant decrease (ca. 50−100% times) of volatility of the first component due to the restricted mobility of the second component suggests that the evaporation of ACN can be tuned by choosing an appropriate RTIL. For instance, the imidazolium-based RTILs with longer alkyl tails (6, 8, 10 carbon atoms) predictably exhibit much smaller self-diffusion. Their glass-like behavior should be a sufficient hindrance for ACN molecules to leave the condensed phase even near a boiling point. On the other hand, the aliphatic tail of RTIL also changes structural inhomogeneity and is known to lead to significant changes in solvation behavior. Our virtual experiment affects all of these time scales equally, while the presence of quite a large lyophobic group may lead to more complicated changes. If these changes are significant, the volatility/evaporation of ACN, in principle, can be drastically affected.

The simulation of the liquid/vapor interface requires to ensure that (a) both phases are well sampled in the box and (b) the gaseous phase in the current box represents a *saturated* vapor. In order to corroborate the accomplishment of these conditions, we derive pressures for smaller (4.2 × 4.2 × 10 nm) and larger (4.2 × 4.2 × 30 nm) boxes containing the 90% [EMIM][BF_4]/ACN mixture at 370 K. This system is selected, since it contains the smallest amount of the ACN molecules (30) at the highest considered temperature. Hence, it is possible that this amount of molecules is not enough to entirely fill the space generating a saturated vapor. If the above conditions are fulfilled for this system, they are true for all other systems as well. The resulting pressures are 0.33, 0.36, and 0.34 bar for 10, 20, and 30 nm box sides, respectively. In turn, the densities of the saturated vapor are 0.33, 0.24, and 0.25 kg m^{-3}. Because the calculated vapor pressures and densities are very similar (compare with Figure 2), we conclude that the interfaces considered in the present work are fully natural.

Further characterization of the [EMIM][BF_4]/ACN and [BMIM][BF_4]/ACN systems is provided in terms of partial specific densities (Figures 3 and 4) along the normal on the liquid/vapor interface. Interestingly, there is a huge gradient of ACN density across the box. At x(RTIL) ≥ 50%, the surface layers are 2−3 times richer in ACN than inner (bulk) layers (Figure 3). This trend does not qualitatively alter with temperature. Obviously, at higher temperatures, the density of liquid phase is somewhat smaller, since a certain fraction of molecules leaves for the vapor phase. The pattern is different for the RTIL-poor mixtures. Both ACN and RTIL are well dispersed throughout the volume, herewith establishing a less sharp liquid/vapor separation line as compared to the RTIL-rich mixtures. Remarkably,

dx.doi.org/10.1021/jz201190j |*J. Phys. Chem. Lett.* 2011, 2, 2499–2503

in the 10% RTIL mixture, [BMIM][BF_4] preserves a more localized condensed phase, additionally confirming that larger ions obstruct vaporization of the more volatile component.

The pure imidazolium-based RTILs do not vaporize over the considered temperature interval, 270−370 K. This behavior is not changed by ACN, notwithstanding the composition of the mixture (Figure 4). The massive, branchy, tightly bound ions ($H_{vap} \sim 130$ kJ/mol) of RTILs remain in condensed phase, while the ACN molecules are vigorously leaving it at the elevated temperatures. This fact allows an easy separation of the two components using, e.g., rectification. One can predict that the trends observed for [EMIM][BF_4] and [BMIM][BF_4] are even more pronounced for their senior homologues. Unlike ACN, the corresponding density distribution along the normal on the interface is uniform. Herewith, in the 10% RTIL mixtures at 330 K and especially at 370 K, the volume occupied by RTIL is subjected to certain deformation. It may look surprising that the vapor pressures (Figure 1) for 10% and 50% RTIL mixtures are similar, while the structure of the interface exhibits certain qualitative differences. This once again demonstrates that there is no straightforward correlation between the structure and transport of liquids and their phase transition regularities. The ionic liquids with lyophobic tails, such as alkyl groups, are often called surfactants, i.e., are expected to possess an elevated concentration on the liquid/vapor interface decreasing surface tension. Figures 3 and 4 show that this is not the case in the RTIL/ACN mixtures of the considered composition. Likely, the surfactant properties appear for the senior imidazolium-based cations and for smaller fractions of RTILs.

To recapitulate, the liquid/vapor interface of the [EMIM][BF_4]/ACN and [BMIM][BF_4]/ACN mixtures over the temperature range 270 to 370 K is studied. It is found that for the RTIL contents of 10, 25, and 50%, the volatility of ACN is almost unaffected by the presence of RTIL. However, if the molar fraction of RTIL grows up to 75% and higher, the volatility of ACN drastically reduces by a few times. The impact of [EMIM][BF_4] and [BMIM][BF_4] are quite similar, since ACN interacts preferrably with the polar imidazole ring rather than with electrically neutral alkyl tails. Meanwhile, the intrinsic transport of RTIL is important for the volatility of ACN. The analysis of partial densities across the interface reveals an unusually significant anisotropy of ACN, which is possible only in the mixtures of the liquids with very different physical chemical properties.

Although the noticeable volatility decrease is quite surprisingly observed only at large molar fractions of RTIL, it favors the applications of the RTIL/ACN mixtures as an electrolyte in the electrochemical devices. A subsequent experimental study is required in order to confirm the reported conclusions.

COMPUTER SIMULATION DETAILS

The MD simulation is carried out using the highly parallel GROMACS 4 molecular simulation engine[19−21] and a few home-made utilities are applied to derive the data from the resulting MD trajectory. The equilibration of the systems is performed in the constant temperature constant pressure (NPT) ensemble, whereas the liquid/vapor interface is simulated in the constant temperature constant volume (NVT) ensemble. The pairwise interaction potentials are applied to treat all the molecular, ionic, and ion−molecular interactions in the systems. All atoms of [EMIM][BF_4] and [BMIM][BF_4] and ACN are represented by separate interaction centers, possessing Lennard-Jones (12,6) parameters and electrostatic charges. The long-range electrostatic forces are treated by the reaction-field-zero (RFZ) method[21] with the cutoff distance of 1.5 nm. Although the force field has been originally parametrized with the variation of the particle mesh Ewald (PME) method,[22] its performance tightly depends of the size of the simulation cell, and hence, is inefficient for the simulation of interfaces. Fortunately, PME can be substituted by RFZ without any loss of accuracy (Table S1), speeding up the calculations by a factor of 1.5. The continuity of the Lennard-Jones potential is assured by using the shifted force method with a switch region between 1.2 and 1.3 nm. The list of the nearest neighbors was updated every 10 steps within a sphere of radius of 1.6 nm.

In order to describe the interionic, ion−molecular, and ion−ionic interations in the [EMIM][BF_4]/ACN and [BMIM][BF_4]/ACN mixtures, we apply our recently developed force field based on the uniformly scaled electrostatic charges[15,23] and AMBER[24,25] Lennard-Jones (12,6) parameters as described and extensively tested versus transport experimental data in refs 15 and 16.

The liquid/vapor interfaces (Figure S1) are represented in the following way. Each [EMIM][BF_4]/ACN and [BMIM][BF_4]/ACN mixture (Table 1) is equilibrated at 300 K employing 10 000 ps MD runs in the NPT ensemble in the periodic cubic box. Next, one of the linear dimensions of the unit MD box is enlarged up to 20 nm, so that liquid/vacuum interface is formed. The subsequent simulations at 270, 290, 310, 330, 350, and 370 K are used to create a liquid/saturated vapor interface due to a natural evaporation of the components. Totally, 66 systems are simulated at this stage, each during 20 000 ps. The first 5000 ps of each run are assigned to the relaxation (interface formation), while next 15 000 ps are used to derive all the analyzed properties.

The saturated vapor pressure is found using the following equation, $\mathbf{P} = 2\cdot(\mathbf{E}_{kin} - \mathbf{G})/V$, where V is the system volume, and $\mathbf{E}_{kin}$ and $\mathbf{G}$ are the tensors of kinetic energy and virial, respectively. The reported pressures act across the interface, i.e., correspond to the saturated vapor pressure only. The partial densities of mass for each component across the liquid/vapor interface are found by dividing the space into 400 equal volume rectangular slices and independently averaging the density inside each of them over the simulation time (15 000 ps). Note that along the liquid/vapor interface all systems are periodic, i.e., the simulated system is a film centered in the unit box. The average vapor densities are calculated from the partial density distributions, integrating the mass density in the vapor phase region. The vapor phase region is defined as a whole space located at least 1 nm apart from the interface.

ASSOCIATED CONTENT

Supporting Information. The Supporting Information includes the depiction of the simulated liquid/vapor interface (Figure S1) and the numerical comparison of particle mesh Ewald and the reaction-field-zero methods for electrostatics (Table S1). This information is available free of charge via the Internet at http://pubs.acs.org/.

AUTHOR INFORMATION

Corresponding Author

*Tel. +1-585-276-5751; e-mail: v.chaban@rochester.edu.

■ ACKNOWLEDGMENT

V.C. is grateful to Florian Dommert (University of Stuttgart) and Julianne Green (University of Rochester) for fruitful discussions. The research is supported in part by the NSF Grant CHE-1050405.

■ REFERENCES

(1) Appleby, D.; Hussey, C. L.; Seddon, K. R.; Turp, J. E. Room-Temperature Ionic Liquids as Solvents for Electronic Absorption-Spectroscopy of Halide-Complexes. *Nature* **1986**, *323*, 614–616.

(2) Blanchard, L. A.; Hancu, D.; Beckman, E. J.; Brennecke, J. F. Green Processing Using Ionic Liquids and CO_2. *Nature* **1999**, *399*, 28–29.

(3) Castner, E. W.; Wishart, J. F.; Shirota, H. Intermolecular Dynamics, Interactions, and Solvation in Ionic Liquids. *Acc. Chem. Res.* **2007**, *40*, 1217–1227.

(4) Wishart, J. F.; Castner, E. W. The Physical Chemistry of Ionic Liquids. *J Phys Chem. B* **2007**, *111*, 4639–4640.

(5) Lu, W.; Fadeev, A. G.; Qi, B. H.; Smela, E.; Mattes, B. R.; Ding, J.; Spinks, G. M.; Mazurkiewicz, J.; Zhou, D. Z.; Wallace, G. G.; et al. Use of Ionic Liquids for π-Conjugated Polymer Electrochemical Devices. *Science* **2002**, *297*, 983–987.

(6) Rogers, R. D.; Seddon, K. R. Ionic Liquids - Solvents of the Future?. *Science* **2003**, *302*, 792–793.

(7) Spohr, H. V.; Patey, G. N. Structural and Dynamical Properties of Ionic Liquids: The Influence of Charge Location. *J. Chem. Phys.* **2009**, *130*, 104506.

(8) Spohr, H. V.; Patey, G. N. Structural and Dynamical Properties of Ionic Liquids: The Influence of Ion Size Disparity. *J. Chem. Phys.* **2008**, *129*, 064517.

(9) Romani, L.; Troncoso, J.; Cerdeirina, C. A.; Navia, P.; Sanmamed, Y. A.; Gonzalez-Salgado, D. Unusual Behavior of the Thermodynamic Response Functions of Ionic Liquids. *J. Phys. Chem. Lett.* **2010**, *1*, 211–214.

(10) Diaw, A.; Chagnes, A.; Carre, B.; Willmann, P.; Lemordant, D. Mixed Ionic Liquid as Electrolyte for Lithium Batteries. *J. Power Sources* **2005**, *146*, 682–684.

(11) Hogan, C. J.; de la Mora, J. F. Tandem Ion Mobility-Mass Spectrometry (IMS-MS) Study of Ion Evaporation from Ionic Liquid-Acetonitrile Nanodrops. *Phys. Chem. Chem. Phys.* **2009**, *11*, 8079–8090.

(12) Kobrak, M. N. Characterization of the Solvation Dynamics of an Ionic Liquid via Molecular Dynamics Simulation. *J. Chem. Phys.* **2006**, *125*, 064502.

(13) Shirota, H.; Castner, E. W. Why Are Viscosities Lower for Ionic Liquids with $-CH_2SI(CH_3)_3$ vs $-CH_2C(CH_3)_3$ Substitutions on the Imidazolium Cations?. *J. Phys. Chem. B* **2005**, *109*, 21576–21585.

(14) Li, H. L.; Ibrahim, M.; Agberemi, I.; Kobrak, M. N. The Relationship between Ionic Structure and Viscosity in Room-Temperature Ionic Liquids. *J. Chem. Phys.* **2008**, *129*, 124507.

(15) Chaban, V. V.; Voroshylova, I. V.; Kalugin, O. N. A New Force Field Model for the Simulation of Transport Properties of Imidazolium-Based Ionic Liquids. *Phys. Chem. Chem. Phys.* **2011**, *13*, 7910–7920.

(16) Chaban, V. V.; Prezhdo, O. V. *Phys. Chem. Chem. Phys.* **2011**, DOI: 10.1039/c1cp22188d.

(17) Bodo, E.; Gontrani, L.; Triolo, A.; Caminiti, R. Structural Determination of Ionic Liquids with Theoretical Methods: C_8mimBr and C_8mimCl. Strength and Weakness of Current Force Fields. *J. Phys. Chem. Lett.* **2010**, *1*, 1095–1100.

(18) Samanta, A. Solvation Dynamics in Ionic Liquids: What We Have Learned from the Dynamic Fluorescence Stokes Shift Studies. *J. Phys. Chem. Lett.* **2010**, *1*, 1557–1562.

(19) Hess, B.; Kutzner, C.; van der Spoel, D.; Lindahl, E. GROMACS 4: Algorithms for Highly Efficient, Load-Balanced, and Scalable Molecular Simulation. *J. Chem. Theory Comput.* **2008**, *4*, 435–447.

(20) Hess, B. GROMACS 4: Algorithms for Highly Efficient, Load-Balanced, and Scalable Molecular Simulation. *Abstr. Pap. Am. Chem. Soc.* **2009**, *237*, 25-COMP.

(21) Berendsen, H. J. C.; van der Spoel, D.; Lindahl, E.; Hess, B.; Groenhof, G.; Mark, A. E. GROMACS: Fast, Flexible, and Free. *J. Comput. Chem.* **2005**, *26*, 1701–1718.

(22) Essmann, U.; Perera, L.; Berkowitz, M. L.; Darden, T.; Lee, H.; Pedersen, L. G. A Smooth Particle Mesh Ewald Method. *J. Chem. Phys.* **1995**, *103*, 8577–8593.

(23) Chaban, V. Polarizability Versus Mobility: Atomistic Force Field for Ionic Liquids. *Phys. Chem. Chem. Phys.* **2011**, *13*, 16055–16062.

(24) Case, D. A. Amber and Its Associated Force Fields: An Update. *Abstr. Pap. Am. Chem. Soc.* **2002**, *223*, U475–U475.

(25) Wang, J. M.; Wolf, R. M.; Caldwell, J. W.; Kollman, P. A.; Case, D. A. Development and Testing of a General Amber Force Field (Vol 25, Pg 1157, 2004). *J. Comput. Chem.* **2005**, *26*, 114–114.